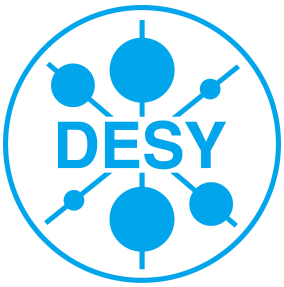

Experimental Investigation of the Phase Stability in Ringwoodite and Wadsleyite

Khachiwan Buakor

Chiang Mai University, Thailand

Supervisor: Dr. Konstantin Glazyrin and Dr. Hanns-Peter Liermann

July 18 - September 7, 2017

Abstract

The objective of this project is to explore the phase stability of olivine polymorphs which are Ringwoodite and Wadsleyite from the high-pressure experiments. Powder mixture of Wadsleyite and Ringwoodite were loaded into a 4-pin diamond anvil cell and were performed at the pressure from 0 to 33.4 GPa and the temperature between 300 to 1305 K. We obtained information on the compression induced behavior of these phases in the metastable region of the phase diagram by X- ray diffraction at P02.2 beamline, PETRA III. Moreover, Ruby(Al_2O_3 doped with Cr^{3+}) and pieces of Tungsten(W) were used as pressure standards. The pressures at an ambient and low temperatures were estimated using the former sensor and with the latter at elevated temperatures we calculated from the tungsten diffraction data by the equation-of-state. The phase stability of Ringwoodite and Wadsleyite was then inspected. We have found that Ringwoodite was stable at all P-T conditions of our study, while Wadsleyite may have converted to Akimotoite.

Contents

1 Introduction

The silicate mantle of the Earth is separated into two major layers called the upper and the lower mantle. This major stratification occurs at the depth of about 670 kilometers and is related with a pressure induced transformation of a mineral Ringwoodite (Mg_2SiO_4) doped by Al and Fe) into minerals ferropericlase ((MgFe) O) and Bridgmanite ($MgSiO_3$ doped by Al and Fe) shown in Fig. 1 [1] [2]. From the phase diagram at about 17.5 GPa or 520 kilometres depth, Wadsleyite transforms into Ringwoodite. At approximately 24 GPa or 660 kilometres, Ringwoodite breaks down to an assemblage of perovskite-structured ((Mg, Fe) SiO_3) and Ferropericlase ((Mg, Fe) O), which marks the beginning of the lower mantle [1].

The aim of this project is to explore the phase stability of polymorphs which are Ringwoodite and Wadsleyite in the metastable regime of the phase diagram. A synthesized powder mixture of Wadsleyite and Ringwoodite was loaded into a 4-pin diamond anvil cell and compressed to 30 GPa. X-ray diffraction was used to measure phase evolution in the metastable regime under varying P-T condition. The high-pressure experiments were performed at P02.2 beamline, PETRA III.

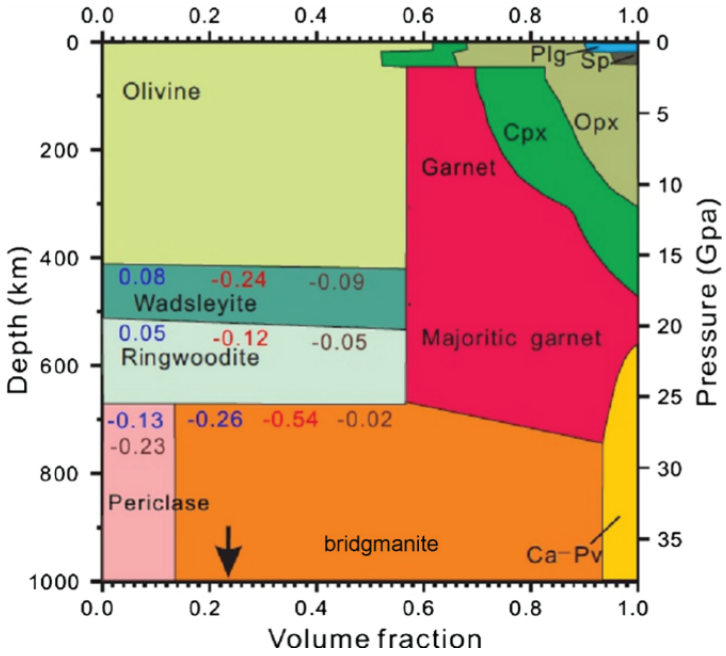

Figure 1: Phase diagram indicating the most abundant minerals of the Earths upper ($<$ 670km depth) and lower mantle ($>$ 670km depth) together with corresponding phase transformations upon compression. Temperature scale is omitted [1] [2].

2 Theory

2.1 X-ray diffraction

X-ray diffraction has been a useful technique for investigating molecular or crystal structures. This phenomena originates from the interaction of X-ray with electron cloud of atoms arranged in a long range manner and results in coherent scattering. Therefore, the physical observation of the X-ray diffraction signal for solids exhibiting long range order is manifested through the Bragg's law,

$$2d \sin(\theta) = n\lambda, \tag{1}$$

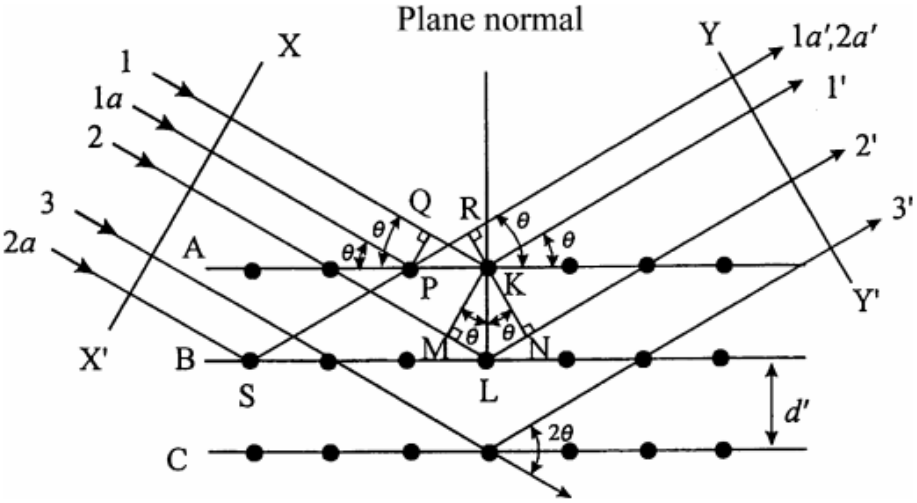

Figure 2: Schematic diagram of diffraction of X-rays by a crystal illustrating the Bragg's law [3].

where n is the order of reflection and 2θ is the diffraction angle shown in Fig. 2. In general, the nth order reflection from a certain crystal plane ($h\,k\,l$) with the interplanar spacing of d could be considered the first-order reflection from a plane [3]. For a cubic system, the relation between the crystal plane, lattice parameter (a) and the interplanar spacing can be calculated as

$$d = \frac{a}{\sqrt{h^2 + k^2 + l^2}} \tag{2}$$

2.2 Equation-of-state at various P-T conditions

An equation-of-state (EoS) is an equation used to described the relationship between pressure, volume and temperature at different conditions of a state close to thermodynamics equilibrium. In Mineral Physics, EoSs are used to determine experimental conditions or unit-cell volumes as functions of different thermodynamic parameters, such as pressure and temperature. There are many approximations which can used to describe material behavior as a function of P and T. In this study, we will use the literature data available for Tungsten and implement the procedure described below. We take an ambient temperature equation of state and use it as reference ($P(V, T_0)$). In order to calculate a pressure at elevated temperature, we add a term described in literature as 'thermal pressure' (ΔP_{th}) [4]:

$$P(V,T) = P(V,T_0) + \Delta P_{th}(V,T). \tag{3}$$

The thermal pressure beyond the $T_0 = 300K$ is conveniently evaluated by integration at constant volume of the thermodynamic identity [4] expressed as

$$\Delta P_{th} = \int_{T_0}^{T} [\alpha K_T]_V \, dT, \tag{4}$$

where α is the thermal expansion and K_T is the bulk modulus. However, αK_T is generally temperature and pressure dependent. Thus, the thermal pressure is then rewritten as [4],

$$\Delta P_{th} = \int_{T_0}^{T} [\alpha K_T](P_0,T)\, dT + \overline{(\partial K_T/\partial T)_V} \left\{ \ln(V/V_0)(T-T_0) + \int_{T_0}^{T}\int_{T_0}^{T} \alpha dT dT \right\}, \tag{5}$$

where $\overline{(\partial K_T/\partial T)_V}$ is an average value for the V-T range of integration. Following the Ref. [4], we can further rewrite the equation as:

$$\Delta P_{th}(V,T) = a_1(T-T_0) + \overline{(\partial K_T/\partial T)_V} \ln(V/V_0)(T-T_0) + a_2(T-T0)^2 + a_3(T-T_0)^3. \tag{6}$$

Considering on the first term of equation 3, we will use the Birch-Murnaghan isothermal equation-of-state. The third-order Birch-Murnaghan equation-of-state is given as [5]

$$P(V) = \frac{3K_{T0}}{2}\left[\left(\frac{V_0}{V}\right)^{\frac{7}{3}} - \left(\frac{V_0}{V}\right)^{\frac{5}{3}}\right]\left\{1 + \frac{3}{4}(K_T' - 4)\left[\left(\frac{V_0}{V}\right)^{\frac{2}{3}} - 1\right]\right\} \tag{7}$$

The choice of the equation-of-state is dictated by the data (i.e.Tungsten) available in literature.

3 Method

3.1 High-pressure diamond anvil cell preparation

High-pressure diamond anvil cell (DAC) is an environment used for material compression and at the same time allowing probing material properties at conditions away from the room pressure (shown in Fig. 3). To prepare the high-pressure cell in this experiment, we prepared a gasket from the rhenium plate (250 μm) and put the starting material and pressure standards (W and Al_2O_3). The starting material (powder mixture of Ringwoodite and Wadsleyite) was synthesized in the multianvil apparatus at 17 GPa and 1100°C by Robert Farla in the Bayerisches Geoinstitute, University of Bayreuth. To measure pressure during the experiment, we used pieces of Tungsten and Ruby as pressure standards. Besides, the high-pressure cell was capable to create high temperature conditions by adding heating circuit and the two thermocouples were used for measuring the temperature. The Baysilone oil was added to be pressure medium. This oil provides good quasihydrostatic conditions at all P-T conditions of our study. We measured the initial pressure plus pressures at moderate temperature of the cell via Ruby chip fluorescence signal by means of visual light spectrometry. By applying pressure to the cell, we shift ambient pressure Ruby chip fluorescence signal (694.29 nm) to higher wavelengths. For pressure calibration at ambient and slightly elevated temperatures, we have used procedure described in Ref. [6] and [7]. The measured initial pressure is about 4 GPa. Finally, the high-pressure cell was installed in the vacuum vessel with the cooling system designed to work with DAC at high P-T conditions (in order to avoid diamond graphitization).

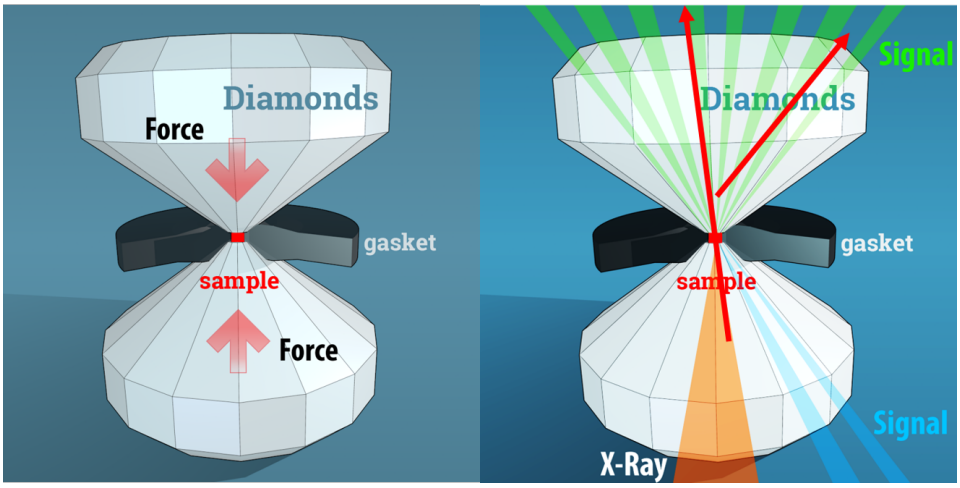

Figure 3: Schematics of high-pressure diamond anvil cell.

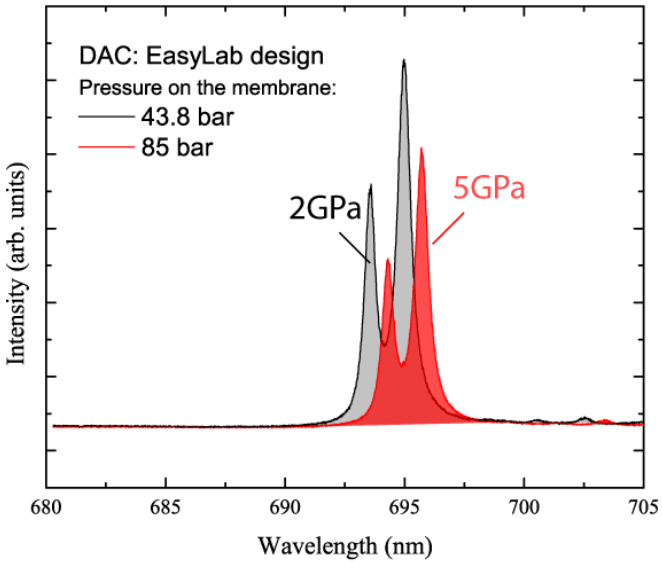

Figure 4: Example of Ruby chip fluorescence signal shifted to higher wavelengths due to applied pressure.

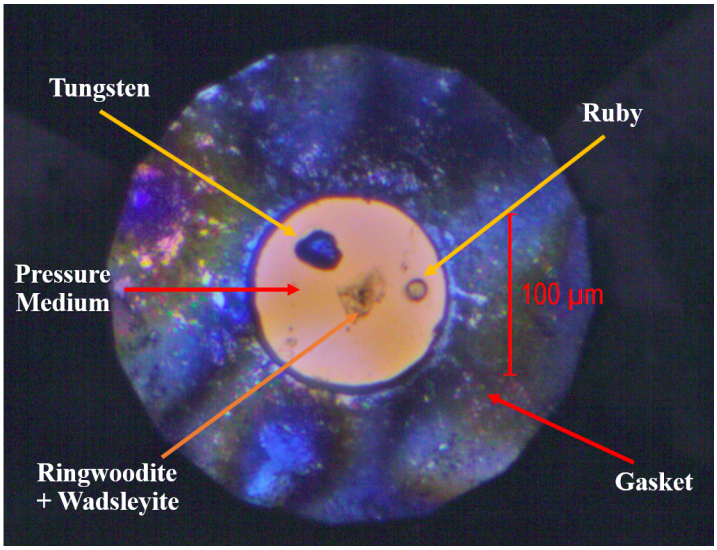

Figure 5: The Ringwoodite and Wadsleyite sample and chips of Tungsten and Ruby used as sensors under the pressure of about 4 GPa.

3.2 X-ray diffraction technique for the high-pressure experiments

The X-ray diffraction experiments were performed at the Extreme Condition Beamline (P02.2), PETRA III. The X-ray generated from the P02.2 insertion undulator device pass through the optical devices (double crystal monochromator, optical slits, focusing elements, such as compound refractive lenses) and reach the sample, which is illustrated by a snapshot of the beamline software shown in Fig. 6. The diffraction pattern was detected at the PerkinElmer XRD1621 detector. Moreover, the position of each sample was inspected and recorded using the microscope which was in addition used for spectroscopy. Here, this microscope was sued for measurement of pressures as reported by the ruby ship. In the experiment, the high-pressure was generated by the membrane and high-temperature was generated from the DC power supply (Agilent 6671: 220A, 8V).

For this experiment, we collected the x-ray diffraction data from both the sample and tungsten during an oscillation of $\pm 5^{\circ}$ and $\pm 10^{\circ}$. The experiments were performed at the pressure from 0 to 33.4 GPa and the temperature between 300 to 1305 K. We used the X-ray with the wavelength of 0.2907 $\mathring{A}$ and the sample-to-detector distance is 433.39 mm. After achieving the required goals, we quenched the sample to ambient temperature. This quenching has resulted in a higher pressure on the sample (36 GPa) shown in Fig. 7.

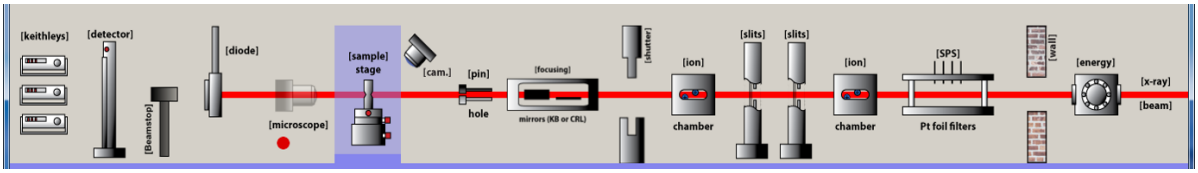

Figure 6: Layout of the Extreme Condition Beamline (P02.2), PETRA III.

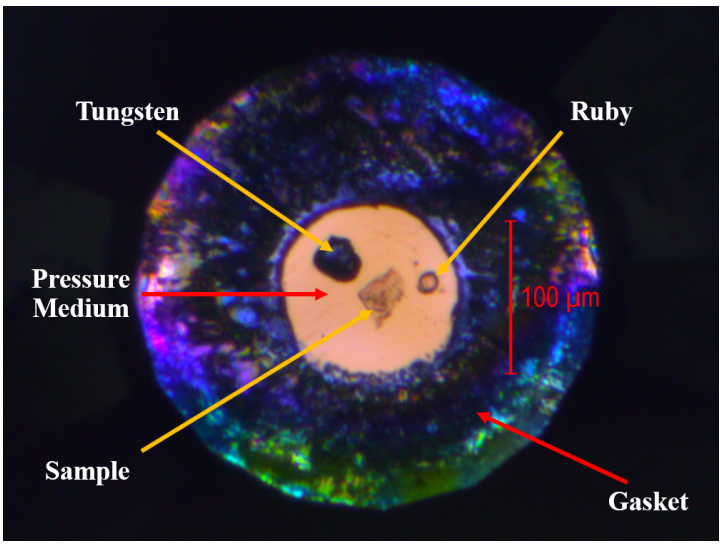

Figure 7: The sample chamber quenched from the high temperature conditions. Slightly deformed gasket illustrates effect of compression on the sample chamber. This example also illustrates compressibility of the pressure medium. Please note the change of sample transparency after annealing.

3.3 Conversion of 2D to 1D X-ray diffraction data

The collected diffraction data were integrated via Dioptas program [8]. We firstly used the data of CeO_2 for calibration. Prior to integration of 2D patterns into 1D, we masked undesirable background signal coming from diffuse scattering from the diamonds and Bragg peaks originating from their single crystal nature. After that we extracted signal from our sample removing a contribution from undesirable scattering (i.e. Compton, X-ray fluorescence).

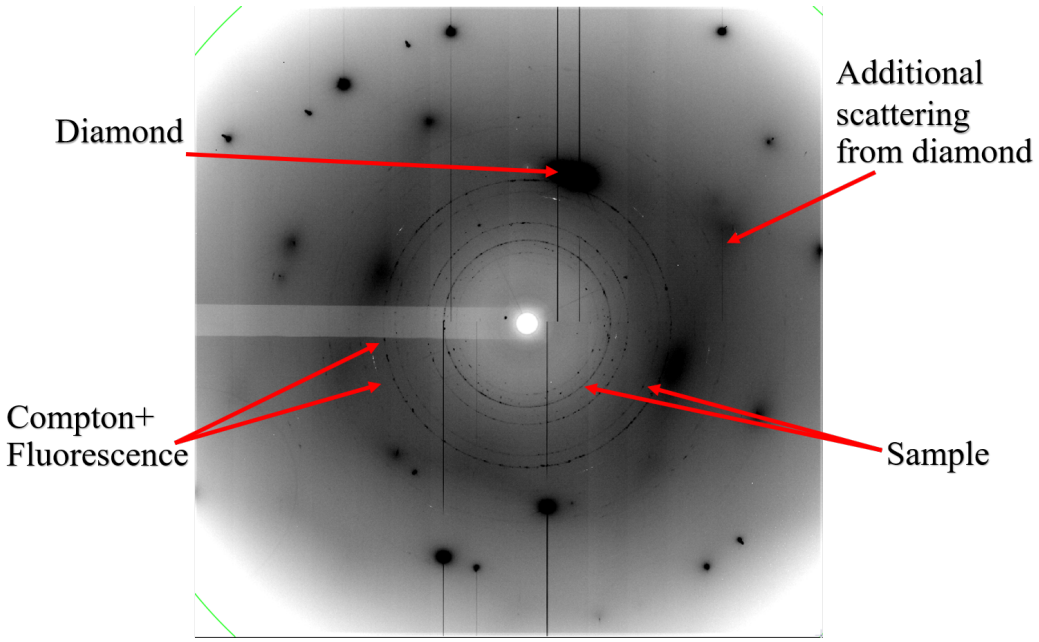

Figure 8: Example of 2D pettern of diffraction data from the Ringwoodite and Wadsleyite sample under the pressure of about 33 GPa.

3.4 Pressure identification from equation-of-state of Tungsten at elevated P-T

During the experiment, we estimated the pressure from fluorescence of Ruby chip .To obtained more precise pressures at higher temperatures, we have to calculate from equation-of-state of Tungsten with a procedure described in Chapter 2.2. We took an ambient temperature equation of state. We include the thermal pressure until the second order rewritten Eq. 6 as

$$\Delta P_{th}\left(V,T\right) = a_1\left(T-T_0\right) + a_2\left(T-T0\right)^2 - \overline{\left(\partial K_T/\partial T\right)}\ln\left(V/V_0\right)\left(T-T_0\right). \quad (8)$$

In this study, we used the parameters $V_0, K_{T0}, K'_T, a_1, a_2$ from Ref. [9] shown in Table 1. Considering on the above equations, we collected the necessary information as a X-ray diffraction signal (V) and as a thermocouple signal (T). A unit cell of Tungsten has cubic shape, so the volume can be calculated from $V = a^3$, where a is the lattice parameters. From the diffraction pattern of Tungsten in Fig. 9, we used WinPLOTR program [10] to detect the position (2θ) of each peak and then to calculate the lattice parameters via Treor program [11].

Table 1: Thermoelastic parameters for Tungsten [9]

Parameter	Value
V_{0T} ($\AA^3$)	31.71 ± 0.02
K_{T0} (GPa)	307 ± 1
K'_T	4.20 ± 0.05
a_1 $\left(10^{-5}K^{-1}\right)$	1.35 ± 0.04
a_2 $\left(10^{-8}K^{-2}\right)$	0.21 ± 0.05
$(\partial K_T/\partial T)_P$ (GPa K^{-1})	0.018 ± 0.001

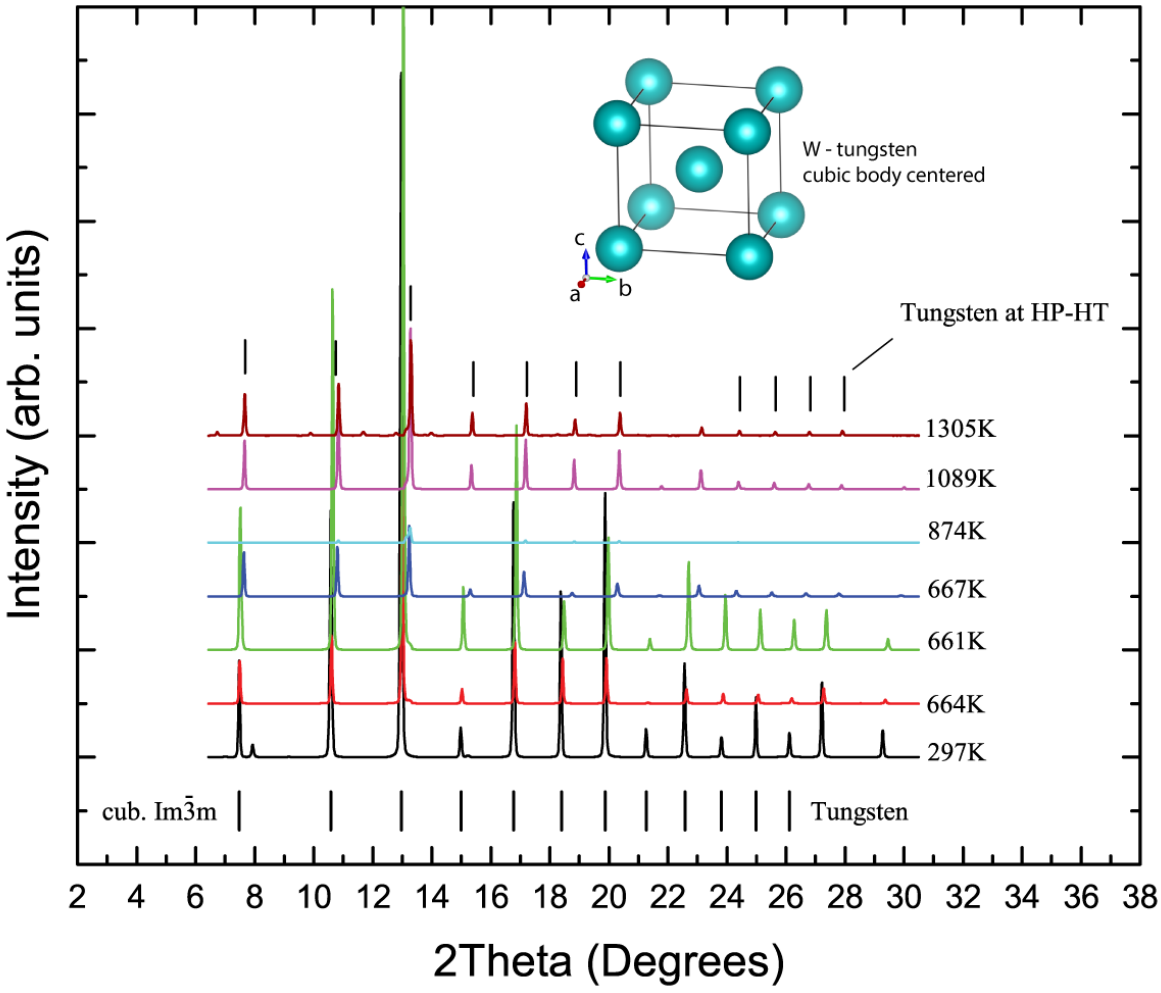

Figure 9: The diffraction patterns of Tungsten piece at different temperature and pressure. Small peaks observed at 1305K correspond to a formation of W2C phase.

After obtaining the volumes, we calculated the pressure at each condition and plotted the relationship between the pressure and volume of Tungsten unit cell shown in Fig. 10. The dash line refer to the reference room temperature Birch-Murnaghan equation-of-state.

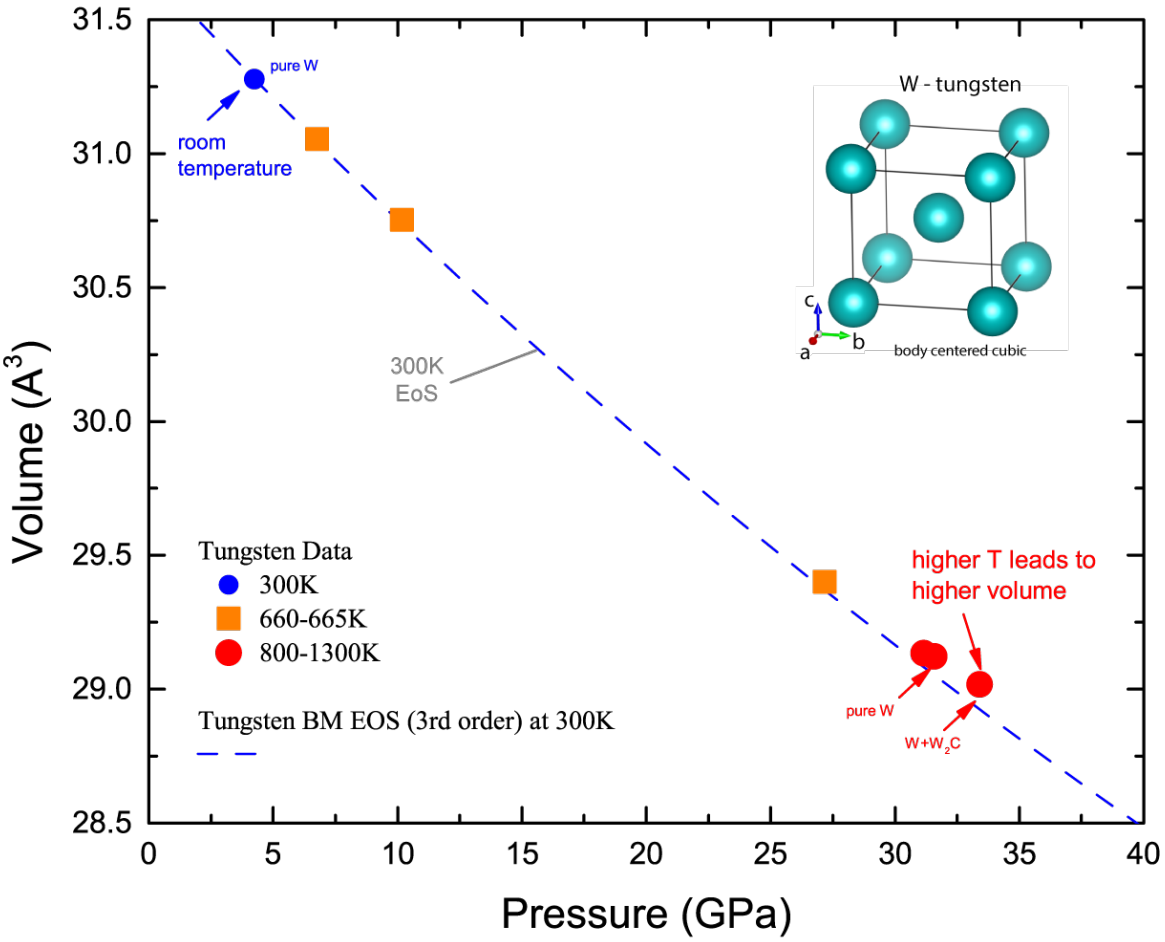

Figure 10: The relation between the calculated volume and pressure of tungsten from the experiment and the Birch-Murnaghan equation-of-state of Tungsten at 300K.

4 Results

As described in the Chapter 3, we got the pressures, temperatures and the diffraction pattern for the sample with starting phase composition: Ringwoodite and Wadsleyite. The phase stability was then investigated. We overlayed the temperature and pressure path of our study on the phase diagram (Fig. 11). The initial goal of the experiment was to test metastability of the Ringwoodite and Wadsleyite versus known stability field of the bridgemanite. For this we chose the path shown in Fig. 11. In order to resolve phase composition of the sample at each P-T conditions we have indexed patterns.

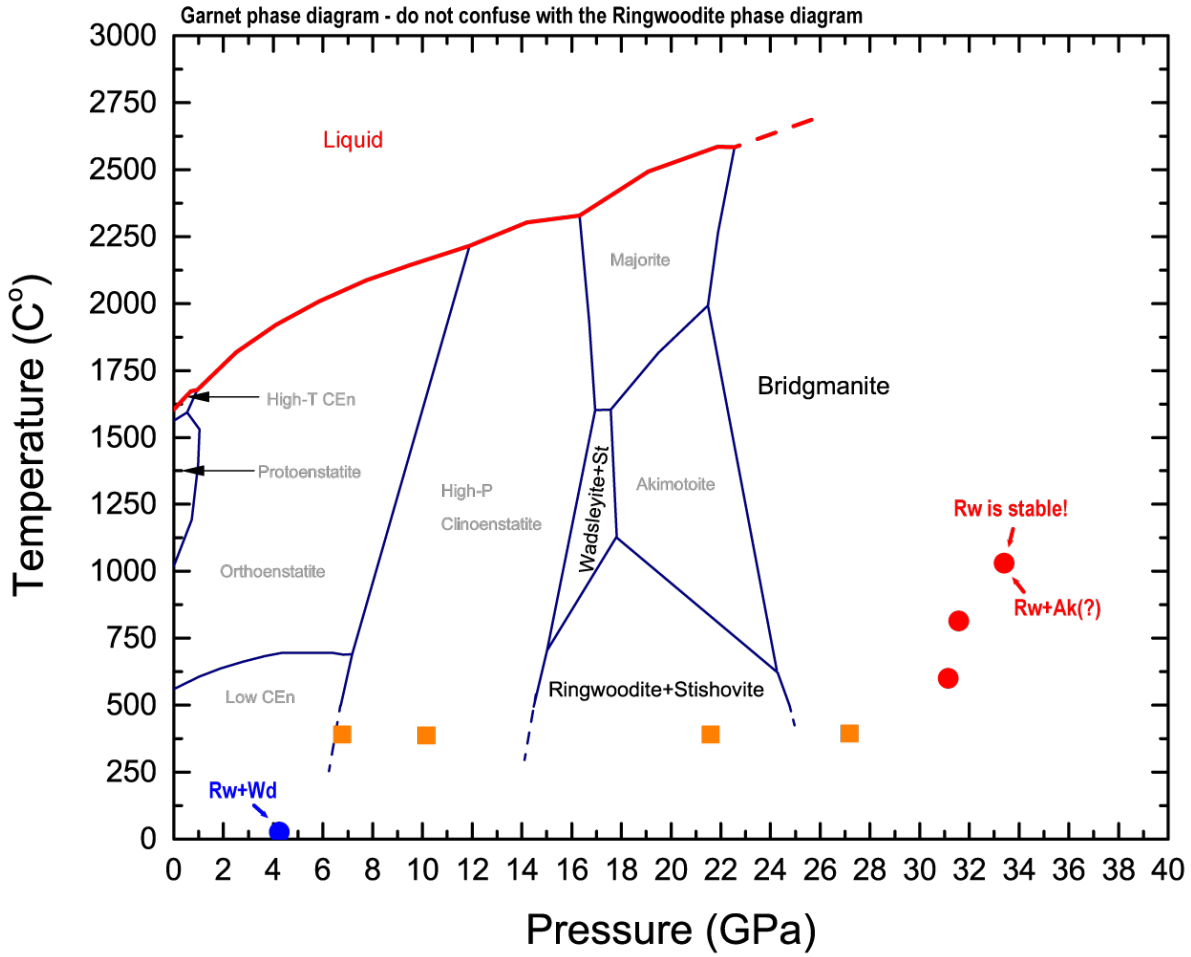

Figure 11: The experimental path overlay with an illustrative text book phase diagram.

Comparing our ambient temperature data with data at high P-T we could come to the following conclusions. A stable, high intensity response from the Ringwoodite indicates its stability even at 1305K and 33.4 GPa. Wadsleyite, on the other hand could convert to Akimotoite (see Fig. 11 and Fig. 12). Unfortunately, the weak signal from Wadsleyite/Akimotoite prevents unambiguous conclusions. However, the probability for such transformation is high and supported by the peaks emphasized in Fig. 12 and the phase diagram shown in Fig. 11.

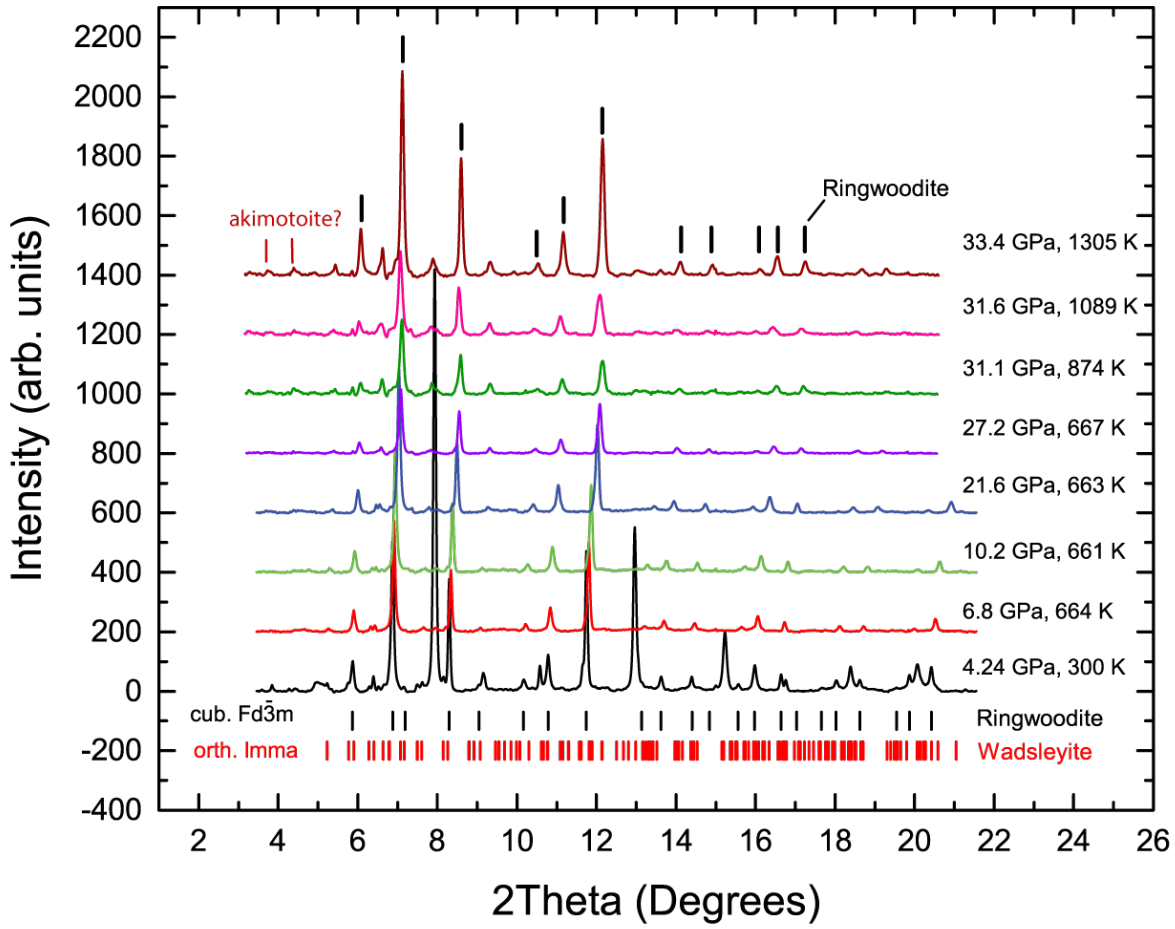

Figure 12: The diffraction patterns collected on the sample under the different pressure and temperature. By means of the tickmarks shown at the bottom of the figure we illustrate a X-ray diffraction response at 4.2 GPa.

5 Conclusion

The phase stability of Ringwoodite and Wadsleyite had been experimentally investigated at high pressure and high temperature. In a contrast to previous studies, for the first time we have investigated the problem of phase stability by approaching the phase stability field of Bridgmanite from a metastable region. The region of metastability is related to the suppressed kinetics preventing the chemical reaction and material disproportionation. This is a first study of the kind paving a way to future studies focused on *in situ* grain growth of lower mantle minerals and the respective crystallographic relations between the corresponding phases. The experiments were performed in a 4-pin diamond anvil cell at the pressure from 0 to 33.4 GPa and the temperature between 300 to 1305 K. Pieces of Ruby and Tungsten were used as pressure standards. The pressures at an ambient and low temperatures were estimated using the former sensor. For elevated temperatures, we calculated from the Tungsten diffraction data by the equation-of-state. By indexing the diffraction pattern from the possible transformed polymorphs, we have found that Wadsleyite may have converted to Akimotoite, while Ringwoodite was stable at all P-T conditions of our study.

Acknowledgement

This research would not be completed, if I did not receive many kind of supports from many kind people. Therefore, I would like to use this section to acknowledge those aids. First of all, I would like to express my gratitude to Dr. Konstantin Glazyrin for your guidances and inspiring me. I have learned many things from working with you. I would like to express my gratitude to Dr. Hanns-Peter Liermann for giving me a chance to work here and supporting for this research. I would like to thank Dr. Anna Pakhomova and other staffs at the P02.2 beamline, PETRA III for your kind support in the experiments. There are also another corporation that I would like to mention that are DESY and Thai DESY Summer Student program organizers from giving this great opportunity to me.

References

[1] D. J. Frost, *The Upper Mantle and Transition Zone*, Elements 4, 171-176, (2008).

[2] Z.Wu, F. Huang and S. Huang, *Isotope fractionation induced by phase transformation: First-principles investigation for Mg_2SiO_4*, Earth and Planetary Science Letters 409, 339-347, (2015).

[3] Y. Waseda, E. Matsubara, and K. Shinoda, *X-Ray Diffraction Crystallography Introduction, Examples and Solved Problems*, Berlin: Springer Berlin, (2014).

[4] I. Jackson and S. M. Rigden, *Analysis of P-V-T Data: Constraints on the Thermoelastic Properties of High-Pressure Minerals*, Physics of the Earth and Planetary Interiors 96, 85-112, (1996).

[5] F. Birch, *Finite Elastic Strain of Cubic Crystals*, Physical Review 71, 809, (1947).

[6] A. Dewaele, M. Torrent, P. Loubeyre and M. Mezouar, *Compression curves of transition metals in the Mbar range: Experiments and projector augmented-wave calculations*, Physical Review B 78, 104102, (2008).

[7] S. Rekhi , L. S. Dubrovinsky and S. K. Saxena, *Temperature-induced ruby fluorescence shifts up to a pressure of 15 GPa in an externally heated diamond anvil cell*, High Temperatures - High Pressures 31, 299, (1999).

[8] C. Prescher, Dioptas, ⟨http://www.clemensprescher.com/programs/dioptas⟩.

[9] K. D. Litasov et al., *Thermal Equation of State to 33.5 GPa and 1673 K and Thermodynamics Properties of Tungsten*, Journal of Applied Physics 113, 133505, (2013).

[10] Ed. R. Delhez and E.J. Mittenmeijer, WinPLOTR, ⟨https://www.ill.eu/sites/fullprof/php/reference.html⟩.

[11] P.-E. Werner, Treor, Department Of Structural Chemistry, Arrhenius Laboratory, University of Stockholm, S-106 91 Stockholm, Sweden.